 doi:10.20944/preprints201809.0008.v1

*Article*

# Proteomics of bronchoalveolar lavage fluid reveals a lung oxidative stress response in murine herpesvirus-68 infection.

**Eric Bortz [1]*, Ting-Ting Wu [2], Parthive Patel [3], Julian P. Whitelegge [4], Ren Sun [2]***

[1] Department of Biological Sciences, University of Alaska Anchorage, Anchorage, Alaska, United States of America.
[2] Department of Molecular & Medical Pharmacology, David Geffen School of Medicine, University of California, Los Angeles, California, United States of America.
[3] Center for Molecular Biology and German Cancer Research Center (DKFZ), University of Heidelberg (ZMBH), Heidelberg, Germany.
[4] Proteomics Division, the Pasarow Mass Spectrometry Laboratory, & Department of Psychiatry & Biobehavioral Sciences & Brain Research Institute, David Geffen School of Medicine, University of California, Los Angeles, California, United States of America.

*Corresponding authors: ebortz@alaska.edu ; 907-786-4858; rsun@mednet.ucla.edu

**Abstract**

Murine herpesvirus-68 (MHV-68) productively infects the mouse lungs, exhibiting a complex pathology characteristic of both acute viral infections and chronic respiratory diseases. We sought to discover proteins differentially expressed in bronchoalveolar lavage (BAL) from mice infected with MHV-68. Mice were infected intranasally with MHV-68. After 9 days, as the lytic phase of infection resolved, differential BAL proteins were identified by 2D electrophoresis and mass spectrometry. Of 23 unique proteins, acute phase proteins, vitamin A transport, and oxidative stress response factors Pdx6 and EC-SOD (Sod3) were enriched. Correspondingly, iNOS2 was induced in lung tissue by 7 days post infection. Oxidative stress was partly a direct result of MHV-68 infection, as reactive oxygen species (ROS) were induced in cultured murine NIH3T3 fibroblasts and human lung A549 cells infected with MHV-68. Finally, mice were infected with a recombinant MHV-68 co-expressing inflammatory cytokine murine interleukin 6 (IL6) showed exacerbated oxidative stress and soluble type I collagen characteristic of tissue recovery. Thus, oxidative stress appears to be a salient feature of MHV-68 pathogenesis, in part caused by lytic replication of virus and IL6. Proteins and small molecules in lung oxidative stress networks therefore may provide new therapeutic targets to ameliorate respiratory virus infections.

**Keywords:** murine herpesvirus-68; MHV-68; bronchoalveolar lavage fluid; BAL; proteomics; oxidative stress.

Preprints (www.preprints.org) | NOT PEER-REVIEWED | Posted: 3 September 2018 doi:10.20944/preprints201809.0008.v1



## 1. Introduction

Respiratory virus infections have the potential to cause significant lung pathology including acute respiratory distress syndrome (ARDS). In addition to the continual burden of disease from respiratory viruses such as influenza types A and B, respiratory syncytial virus (RSV), parainfluenza viruses, and adenovirus, recently emerged coronaviruses responsible for Middle East (MERS-CoV) and severe acute (SARS-CoV) respiratory syndromes, H5N1 and H7N9 pathogenic avian influenza viruses, pandemic swine-origin (H1N1) influenza, and human metapneumovirus target the human lungs [1-7]. Co-morbid, underlying pulmonary medical conditions including asthma, chronic obstructive pulmonary disease (COPD), and tuberculosis (TB), are associated with severe respiratory virus infections [8-11]. Moreover, chronic pulmonary diseases such as asthma, COPD, and idiopathic pulmonary fibrosis (IPF), might have an infectious viral component to their onset and/or pathogenesis. The gammaherpesviruses Kaposi's sarcoma-associated herpesvirus (KSHV/HHV-8) and Epstein-Barr virus (EBV) have been detected in the lung tissue of patients with IPF and AIDS-related lymphocytic interstitial pneumonias [12-14]. In contrast, a murine gammaherpesvirus is protective in mice challenged with lethal influenza A virus, suggesting immunomodulatory roles for gammaherpesviruses in pathogenesis of lung infections [14]. Thus, application of new genomics technologies for understanding respiratory virus infections under isogenic host conditions might yield deeper insight into the pathological changes that occur in virus infection of the mammalian lung, and provide targets for diagnostic biomarkers or therapeutic intervention.

Murine gammaherpesvirus-68 (MHV-68) infects the lungs of wild and laboratory mice, productively infecting type I and II alveolar epithelial cells, macrophages, and dendritic cells (DC) [15,16]. MHV-68 exhibits characteristics of both acute and chronic respiratory pathogens. Even though MHV-68 can inhibit type I interferon secretion by DC [17], the lungs of mice infected by the virus eventually exhibit discernable pathology, including usual interstitial pneumonia (UIP) with diffuse alveolar damage (DAD), and infiltration of inflammatory cells [16,18,19]. MHV-68 infection induces pro-inflammatory chemokines including MCP-1, MIP-1a, MIP-1b, IP-10 and RANTES [20] in the lung, and interleukin-6 (IL6) and type II interferon (IFN-gamma in the draining (mediastinal) lymph nodes [21]. Acute infection is resolved and lytic replication of virus cleared from the lungs in a CD8 cytotoxic T-lymphocyte (CTL-) and type I alpha/beta-interferon receptor (IFNAR)-dependent manner [22,23]. Clearance also requires CD80/CD86 antigen presentation [24], IFN [25], and some degree of CD4+ T-cell help reliant on PKCθ [26]. However, as gammaherpesvirus infection progresses into latency, MHV-68 DNA remains detectable in the lung parenchyma, recapitulating a chronic disease characterized by increased interstitial collagen deposition, immune deregulation, and fibroblast proliferative events similar to those thought to occur early in the development of idiopathic pulmonary fibrosis (IPF). This chronic pathology phenotype is more clearly observed under experimental conditions where the lungs have been insulted prior to infection by an agent that induces pulmonary fibrosis [27], such as fluorescein isothyocyanate (FITC), or in mice deficient in immune responses, such as interferon gamma receptor-null mice [15].

The pro-inflammatory cytokine IL6 is thought to be involved in host response to respiratory infections. IL6 is upregulated in ARDS caused by bacterial pneumonias in human patients [28], and in LPS-treated human lung cells infected with RSV [29]. While no differences in viral life cycle, cytokine profiles, nor cytotoxic T-cell responses were observed in MHV-68 infection of IL6-deficient

Preprints (www.preprints.org) | NOT PEER-REVIEWED | Posted: 3 September 2018 doi:10.20944/preprints201809.0008.v1



mice, IL6 does appear to regulate natural killer (NK) cells responding to MHV-68 infection [30]. Interestingly, KSHV also encodes a viral homologue of IL6 (vIL6) with distinct signaling activity during lytic infection [31,32]. To study the role of exogenous expression of this cytokine in gammaherpesvirus infection of the lung, we constructed a recombinant MHV-68 virus expressing murine IL6.

Proteomics analysis of bronchoalveolar lavage (BAL) fluid has emerged as a new approach to understand pathophysiological events occurring in acute, infectious, malignant or chronic obstructive lung diseases, both in human patients and animal models [33,34]. BAL is a rich source of information about lung cytokine and chemokine responses, inflammatory proteins, and immune cells present or infiltrating into the alveolar lumen. In proteomics studies, proteins isolated from BAL fluid have been typically analyzed by isoelectric focusing followed by 2-dimensional electrophoresis (IEF/2DE), or by multidimensional protein identification technology (MudPIT), allowing for identification of differentially-expressed proteins secreted or released via pathological processes into the alveolar lumen. These studies have begun to add a new dimension into characterization of human or mouse physiological responses to acute lung injury (ALI) [33], ARDS [35,36], and diffuse interstitial lung diseases including IPF [37], COPD [38], and oxidative or toxicological damage to the lung [39,40]. In animal models of infectious diseases, BAL has revealed lung cytokine and chemokine profiles and immune cell populations in response to virus infections [15,20,41]. For a monkeypox virus infection model in macaques [42] and three pathogens in mouse infection models, RSV [43], *Staphylococcus aureus* [44,45], and *Klebsiella pneumoniae* [46], proteomics analyses of BAL have identified inflammatory proteins and revealed commonalities in infectious pulmonary pathophysiology. Analysis of mouse BAL by IEF/2DE showed a suppression of antioxidant and oxidative stress proteins during RSV infection [43]. However, no analysis using differential IEF/2DE proteomics in MHV-68 infection of the mouse lung have been published to date.

As many human viruses infect the lung, understanding proteins present in BAL using MHV-68 as a model may uncover novel aspects of the mammalian host's response to pulmonary viral infections. Using proteomics, we have identified mouse BAL proteins differentially up-regulated by virus infection and overexpression of a cytokine (IL6). Proteins involved in acute phase response, oxidative stress responses, and vitamin A signaling were salient in the MHV-68 infected lung. Interestingly, these proteins are induced by 9 days post-infection (d.p.i.), as the initial phase of MHV-68 infection resolves and lytic replicating virus is cleared from the lungs by T-cell mediated host responses [20,23]. The experimental protocol herein demonstrates the feasibility of differential BAL proteomics to characterize less-abundant, highly regulated host factors in BAL fluid.

## 2. Materials and Methods

**Viruses and cell cultures.** Wild-type (WT) MHV-68, MHV68/IL6, and RFP/MHV-68 viruses in this study were all titered by plaque overlay assay on BHK21 cells as previously described [65,110]. Recombinant viruses were generated by co-transfection of MHV-68 genomic DNA and a PCR-generated cDNA encoding the gene to be inserted flanked by MHV-68 sequences corresponding to the MHV-68 genome. MHV68/IL6 virus was generated by homologous insertion of murine cDNA encoding interleukin-6 (IL6) driven by CMV immediate early (IE) promoter-enhancer into an intergenic locus near the 5′ end of the MHV-68 genome [111]. RFP/MHV-68 virus was generated in a similar manner whereby a cDNA encoding red fluorescent protein (RFP) driven by CMV IE

Preprints (www.preprints.org) | NOT PEER-REVIEWED | Posted: 3 September 2018 doi:10.20944/preprints201809.0008.v1



promoter-enhancer was inserted into the ORF28 locus. The ORF28 gene is dispensable for infection of cultured cells and *Mus musculus* models of MHV-68 infection [112]. Recombinant viruses were selected by plaque-purification, viral DNA was purified and screened for cDNA insertion into expected loci by PCR and restriction fragment digestion followed by Southern blotting, as has been described [110,111,113]. During lytic infection in NIH3T3 cells, expression of IL6 from MHV68/IL6 virus was confirmed by Western blotting and ELISA; for RFP/MHV-68, expression of RFP was observed by epifluorescent microscopy. To probe for reactive oxygen species (ROS), murine NIH3T3 or human A549 cells were infected with RFP/MHV-68 (m.o.i=1 or 5) and at 4 or 20 h.p.i., cells were rinsed in cold 1xPBS, incubated 5 minutes at 37°C in the dark in 1xPBS containing 5µM 5/6-carboxy-2',7'-difluorodihydrofluorescein diacetate ($H_2DF_2DA$), a compound that exhibits superior photostability compared to other fluorescein derivatives (Invitrogen, Carslbad, CA), washed in 1xPBS, and then imaged in an epifluorescent microscope. ROS inducing compounds $H_2O_2$ or paraquat (10µM) were employed as positive controls for $H_2DF_2DA$ fluorescence. For examining ROS effects on viral titer, NIH3T3 cells were infected with RFP/MHV-68 (m.o.i.=0.25) in the absence or presence of 1mM soluble glutathione (GSH) or 2-25µM paraquat in media. After 20 hours, culture supernatants were diluted ½, 1/10, or 1/100, used to re-infect fresh NIH3T3 cells, and RFP fluorescence observed 20 h.p.i. by epifluroescence microscopy.

**Mouse infections with MHV-68 and MHV68/IL6 viruses.** All *in vivo* mouse experiments were conducted at UCLA in a dedicated animal facility under approved UCLA IACUC ethical guidelines for laboratory animals in research. For 12-week old male C57/BJ6 mice (Charles River Laboratories, Wilmington, MA) were anesthetized with 0.1ml (100mg/kg) ketamine by intraperitoneal (i.p.) injection, and then inoculated with 20µl DMEM or infected intranasally (i.n.) with $5x10^5$ pfu of WT MHV-68 or MHV68/IL6 virus diluted in 20µl DMEM. Mice in each experimental group were housed separately until sacrifice at 6, 7, or 9 d.p.i., when mice were anesthetized and sacrificed under anesthesia by i.p. injection of 0.1ml ketamine. Mice were subsequently dissected and subject to either whole-lung harvest with snap-freezing of tissue in liquid $N_2$ and determination of viral titer as described [65,111], or bronchoalveolar lavage (BAL) thrice with 1.4 ml sterile 1xPBS via a rounded 21G syringe inserted by tracheotomy and affixed with suturing thread. BAL fluid was centrifuged immediately (2000*x*g, 15', 4°C) to separate soluble, supernatant phases and cell/debris pellet. Supernatants were kept at -80°C until processing. Cell pellets were resuspended in 50µl 0.5% FBS DMEM containing 1mM EDTA, and monocytes in 5µl aliquots were counted by trypan blue exclusion test with a hemacytometer. Aliquots of cell fractions (5µl) were also analyzed by thin smear on poly-lysine coated glass slides followed by fixation and eosin/hematoxylin staining with Hema3 (ThermoFisher Scientific, Waltham, MA) according to the manufacturer's instructions, and light microscopy.

**BAL fluid processing.** Aliquots of BAL fluid supernatants were used for Sircol collagen assay, viral DNA detection by quantitative PCR, and protein detection by Western blotting. The remainder of BAL fluid supernatants were pooled for each experimental condition, precipitated in 95% acetone at -20°C for 2h, centrifuged (4°C, 15', 20000*x*g), and then resuspended in binding buffer to reduce abundant immunoglobulins and albumin by Aurum column binding and elution (Bio-Rad, Hercules, CA) according to the manufacturer's instructions. Eluants were re-concentrated and desalted by 4:1 acetone (95%, ice-cold) precipitation for 2h, centrifuged (4°C, 15', 20000*x*g), and resuspended in isoelectric focusing (IEF) buffer. Bradford assay was used to quantify protein concentration prior to and post-processing [64], and SDS-PAGE with SYPRO-Ruby staining was used to observe depletion of abundant albumin bands.

**Sircol collagen assay.** For lung tissue collagen assay, 0.05g lung tissue was homogenized in 0.5 M acetic acid (1ml) containing 7.5 mg pepsin, and rotated for 24 h at 4°C. Samples were briefly centrifuged to pellet debris, and 100µl of each supernatant was assayed for collagen by Sircol assay as described by the manufacturer (BioColor Ltd., UK). For measuring soluble collagen in BAL fluid, aliquots of 25µl were subjected to Sircol assay. Collagen concentration was determined by absorbance at 540nm in a spectrophotometer and titration according to standard curves generated for lung tissue and BAL fluid.

**Catalase assay and immunoblotting.** NIH3T3 cells were lysed in passive lysis buffer and protein content was normalized by Bradford assay as described previously [64], and lysates subjected to catalase activity assay (Sigma, St. Louis, MO) according to the manufacturer's instructions. A standard curve was generated with controlled quantities of $H_2O_2$. $H_2O_2$ treatment for 24h yielded only a minimal induction of catalase activity in this assay. For Western blots, protein lysates separated by SDS-PAGE were Western blotted and probed with specific polyclonal anti-ORF65/M9 antisera or anti-catalase antibody (Calbiochem, San Diego, CA) with HRP-linked secondary and electrochemiluminescent detection as described [110].

**PCR.** For quantitative RT-PCR, total RNA was isolated from mouse lungs 7 d.p.i. and reverse transcribed into cDNA as described [65,111]. Primers to specific murine genes (described in Supporting Information Table S2) were used to amplify transcript cDNA and relative transcript copies determined by CT method with actin internal control by SyberGreen (Applied Biosystems, Carlsbad, CA) real-time detection on a LightCycler thermocycler (Roche, Indianapolis, IN). Significance of relative gene expression was determined by unpaired, 2-tailed t-test. Viral DNA representing viral genome copy number was determined by qPCR with primers specific to MHV-68 genomic ORF65/M9 or ORF57 loci as previously described [110,113].

**IEF, 2D-PAGE, spot mapping and densitometry**. Eluted BAL proteins (300µl) were resuspended in IEF buffer containing ampholytes covering the pH 3-10 range (Bio-Rad, Hercules, CA). Samples passively loaded on rehydrated, immobilized 11cm nonlinear pH 3-10 gradient IPG strips (Bio-Rad) and then focused by *p*I for 18h ramping over 6h to a maximum current of 70000V-h in a Protean IEF Cell (Bio-Rad). Strips were re-equilibrated for 30′ in DTT and then iodoacetamide buffers, and proteins separated by mass in denaturing 8%-16% gradient Criterion 2D-PAGE (Bio-Rad). 2D gels were briefly incubated in 10% methanol/5% acetic acid, rinsed in $ddH_2O$, and stained 3h with SYPRO-Ruby (Invitrogen). Gels were imaged under UV light and analyzed to identify differentially-expressed protein spots. Proteins resolved in pH 4-7 range were sufficiently separated for spot mapping across gels using an integrated ProteomeWorks *PD Quest 7.1* imager and software (Bio-Rad) with manual spot validation. Spots were quantified by peak cross-sectional densitometry using *ImageQuant* (GE Healthcare, Piscataway, NJ), and normalized to an average of oxytocin-receptor (spot 13) and a common major form of eluted albumin (spot 5) relative to gel image background density. A total of 89 abundant differential spots across the three experimental conditions were excised and in-gel digested in Trypsin Gold MS (Promega, Madison, WI), and alkylated peptides were extracted, dried and stored at -80°C as described previously [52] for mass spectrometry identification.

 doi:10.20944/preprints201809.0008.v1



**Mass spectrometry.** Tryptic peptide digests of proteins were separated on a reverse phase column and identified by tandem micro-LC/MS-MS and in some cases, by MALDI-TOF mass spectrometry, with sample handling as described previously [114,115]. BSA (5pmol) digested in Trypsin Gold was used to generate positive control spectra for LC/MS-MS and MALDI-TOF experiments, respectively. Briefly, MS-MS spectra were captured on an AB Sciex Qstar quadrapole XL hybrid TOF LC/MS-MS (Applied Biosystems) with tandem peptide ion fragmentation running in Information Dependent Acquisition (IDA) mode. Peptide and fragment a-, b- and y-series ions spectra were analyzed by *Mascot* software (Matrix Sciences, Boston, MA) with peptide tolerance set at <0.5Da, MS/MS tolerance <0.8Da, charge states +1/+2/+3/+4, 1 tryptic digest miss allowed, oxidation of Cys and Met, with peptide identification by search against the predicted mouse proteome at NCBI and EBI reference databases. From tryptic digests of excised spots, 44 yielded peptide data identifying 23 unique proteins. Positive identification cutoffs were determined on a case-by-case basis with expectation scores $<10^{-2}$ ($p<0.05$, for 20 hits), or ($p<0.1$, for 3 hits), considering multiple peptide hits and supporting MALDI-TOF data in assignment. Another 7 spots did not meet a significance cutoff or poorly matched predicted *p*I and MW, including annexin A5, hemoglobin fragment, triose phosphate isomerase, matrix metalloproteinase 8, serpin b 3d, and collagens I and VI (not shown).

For MALDI-TOF, aliquots of peptide digests were mixed with 200x proportion of -cyano FHSA matrix dissolved in 70% acetonitrile and 0.1% TFA and spotted with for laser ionization and data capture with a low mass gate (500Da) on an AB Sciex Voyager MALDI-TOF running *PD Quest* software (Applied Biosystems). MALDI peptide data were searched against the mouse proteome using *Aldente* software [116], with predicted *p*I and molecular mass data estimated from 2D-PAGE spots.

**Bioinformatics analyses.** Functional enrichment among the set of proteins discovered in enriched BAL fluid was analyzed by *Ingenuity Pathways Analysis* (IPA 7.6, Ingenuity Systems Corp., Redwood, CA) as has been described [74]; IPA categories were tested for significance by a Benjamini-Hochberg test for false discovery [117]. BAL protein functions were also analyzed by Database for Annotation, Visualization, and Integrated Discovery (DAVID) algorithms [60] to assess significant Gene Ontology (GO), InterPro (IPR), and Protein Information Resource (SP_PIR) annotations. A subnetwork of oxidative stress-associated molecules was discovered and extracted using IPA with manual literature curation to construct a network model [62]. Amino acid sequences of human and mouse TNFAIP8 family proteins were obtained from UniProt database and CLUSTAL multiple sequence alignments performed and formatted using MAFFT FFT-NS-2 v5.731 [118].

## 3. Results

### *3.1. Recovery and characterization of BAL fluid from mouse lungs infected with MHV-68*

An unexpected observation regarding MHV-68 infection of laboratory mice was that MHV-68 infection could exacerbate pulmonary fibrosis [15,27,47-50]. Thus we also sought to identify proteins induced by MHV-68 infection accompanied by co-expression of murine IL6, a pro-fibrotic cytokine. C57/BJ6 mice were inoculated intranasally (i.n.) with DMEM, or infected with a high titer of WT MHV-68 or a recombinant MHV-68 virus co-expressing murine interleukin-6 (IL6) from a constitutive promoter. To discover secreted or extracellular proteins in virus infection of the mouse lungs, we developed an experimental procedure to analyze the BAL fluid proteome (Figure 1A). At 6 and 9d.p.i., BAL fluid was collected and analyzed for cells, protein, soluble collagen, and viral DNA

 doi:10.20944/preprints201809.0008.v1



content. At 6d.p.i., MHV68/IL6 showed significantly more soluble type I collagen in BAL fluid than WT MHV-68 infection; by 9d.p.i., soluble type I collagen was significantly higher in BAL fluid from both WT and MHV68/IL6 infection in comparison to uninfected control (Figure 1B). Subsequent analysis focused on the 9d.p.i. timepoint, for which soluble type I collagen levels in BAL were similar between WT virus and MHV68/IL6, and good resolution of proteins by IEF/2DE was achieved. Both protein concentration and mononuclear cellularity in BAL fluid were substantially higher in infected *v.* uninfected mice at 9d. p.i., and viral DNA was detected (Figure 1C). Viral DNA and MHV-68 viral capsid antigen ORF65/M9 was also present in clarified BAL fluid (Figure S1). The numbers of BAL mononucleocytes (Figure S1) recovered in our study (Figure 1C) was similar to a previous report that undertook a detailed phenotypic characterization of mononuclear cell infiltrates, chemokines and cytokines in MHV-68 infection of the lungs [20].

**Fig. 1**

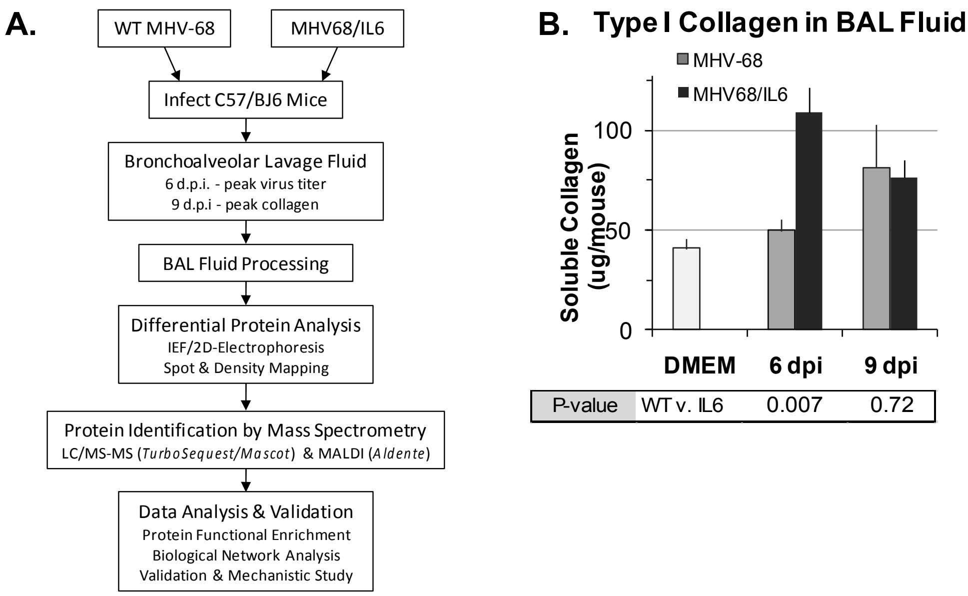


**C. Characteristics of Bronchoalveolar Lavage (BAL) Fluid**

| Mouse Inoculum | Day | Mice in Pool | Protein Recovered BALF (ug) | Protein Recovered Eluate (ug) | Viral DNA | Cells |
|---|---|---|---|---|---|---|
| **DMEM** | 9 | 3 | 375±102 | 150±16 | nd | 1.8 |
| **MHV-68** | 9 | 2 | 633±197 | 204±20 | 1.14 | 3.1 |
| **MHV68/IL-6** | 9 | 2 | 660±124 | 203±20 | 0.14 | 3.8 |

**Figure 1.** Analysis of bronchoalveolar lavage (BAL) fluid from MHV-68 infection of the mouse lung. **(a)** Overview of differential proteomics analysis of proteins induced in BAL by virus infection. Wild-type (WT) MHV-68 or MHV68/IL6 virus infection, BAL fluid processing, protein spot identification, and protein data analysis scheme. BAL fluid processing removed cells, immunoglobulins, excess albumin, and salts, enriching recovered elutant for less-abundant proteins. **(b)** Collagen production in MHV-68 infection of the mouse lung is exacerbated by lytic expression of IL6. C57/BJ6 mice were mock infected with DMEM or infected intranasally with 5x10$^5$ pfu of WT MHV-68 or MHV68/IL6 virus. Type I collagen in BAL fluid in MHV-68 and MHV68/IL6 infection

*Preprints* (www.preprints.org) | NOT PEER-REVIEWED | Posted: 3 September 2018 doi:10.20944/preprints201809.0008.v1



was measured at indicated times post-infection by Sircol assay; *p*-value of fold induction estimated from unpaired, 2-tailed t-test. **(c)** Characteristics of bronchoalveolar lavage (BAL) fluid. BAL fluid recovered 9 d.p.i. from C57/BJ6 mice inoculated as above was processed to remove cells, salts, abundant serum proteins and immunoglobulins. Average protein concentration was measured by Bradford assay; average viral DNA copy number (x$10^5$ cp) in BAL measured by q-PCR; average mononuclear cellularity (x$10^5$ cells) measured by trypan blue hemocytometry.

### *3.2. Differential proteomics analysis of BAL fluid*

Recovered BAL fluid from 9d.p.i. was pooled for each experimental condition (DMEM, WT MHV-68, or MHV68/IL6, respectively), and processed to remove cells and reduce abundant immunoglobulins, albumin, and salts. Reduction of the most abundant proteins in biofluids is a common approach for reducing proteome complexity to enrich less abundant but biologically interesting proteins [51]. Enriched BAL proteins were analyzed by comparative 2-dimensional gel electrophoresis (IEF/2DE) display (Figure 2). WT MHV-68 and MHV68/IL6 infection induced a considerably more complex proteome than DMEM-inoculated control mice. Prominent constitutive and differentially-expressed orthologous proteins were mapped and identified by LC/MS-MS and/or MALDI mass spectrometry. We mapped 39 spots in the pH 3-7 range, and identified **23** unique proteins, of which 20 proteins had high significance scores ($p$<0.05) and 3 proteins (A2MP, OxtR, and Tnfaip8l2) had marginal scores ($p$<0.1) for at least 2 peptide matches (Supporting Information Table S1). Even though viral ORF65/M9 antigen was detected by Western blot in clarified BAL fluid supernatants (Figure S1), peptides matching MHV-68 virion proteins [52] in enriched BAL fluid data did not reach the significance cutoff (data not shown). Of the proteins identified, 13 were induced by WT MHV-68 infection (6 strongly), and 5 were markedly upregulated in the context of MHV68/IL6 (Figure 2D). Another four proteins showed a reduced abundance in the context of either virus infection in comparison to DMEM-treated, uninfected control mice (Figure 2D and Table S1).

Preprints (www.preprints.org) | NOT PEER-REVIEWED | Posted: 3 September 2018 doi:10.20944/preprints201809.0008.v1



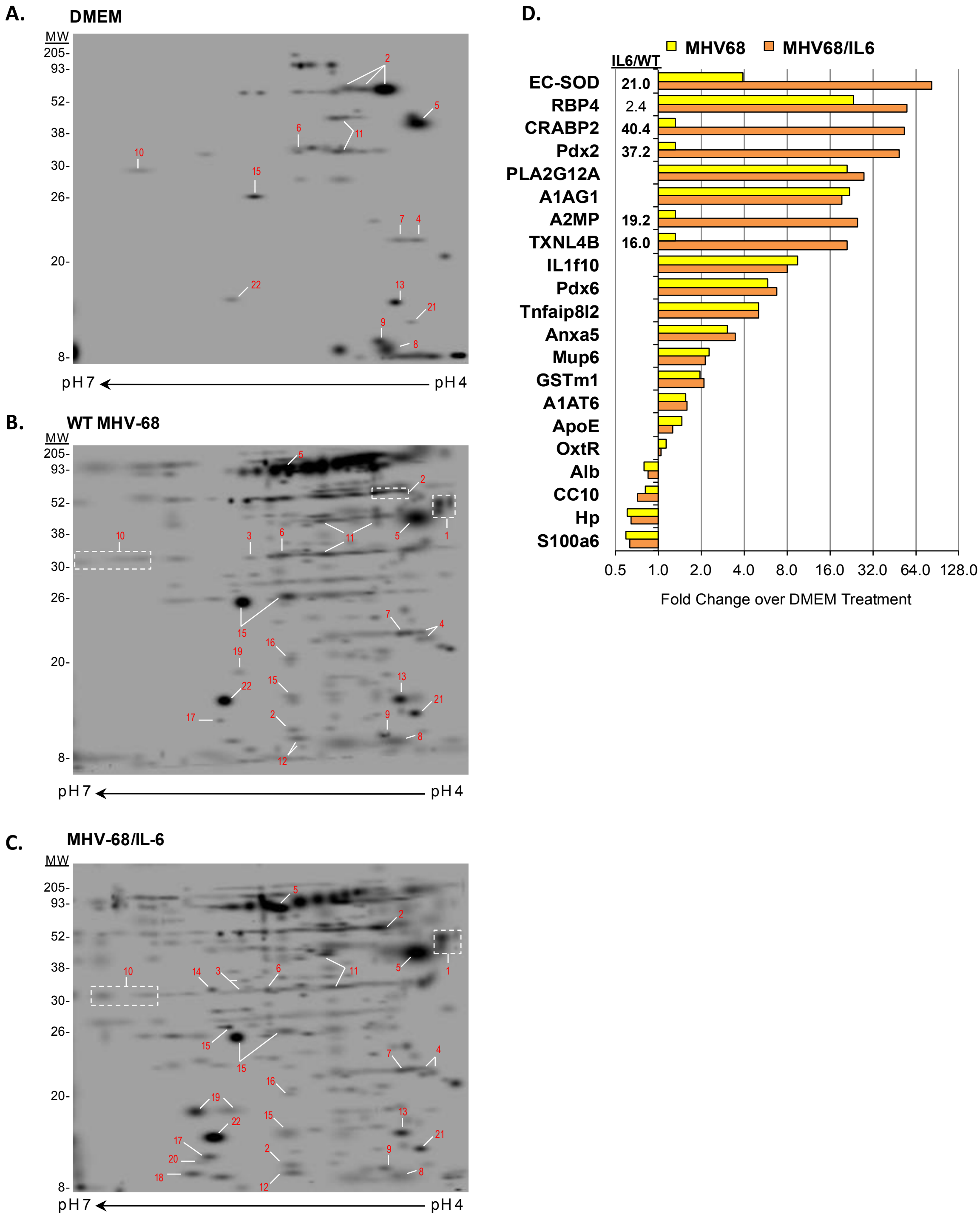


**Figure 2.** Enriched BAL proteome from mice infected with MHV-68 viruses. Mice were intranasally inoculated with DMEM **(a)**, or infected i.n. with 5x10$^5$ pfu of WT MHV-68 **(b)** or MHV68/IL6 virus **(c)**. BAL was collected from mouse lungs 9d.p.i., pooled, and processed to enrich for less abundant proteins as described in Methods. Eluted BAL proteins were separated by isoelectric focusing followed by 2D-PAGE and SyproRUBY staining. Proteins resolved in pH 4-7 range were sufficiently separated for spot identification, excision, and tryptic digestion for protein identification by MALDI and/or LC/MS-MS. Spots were quantified by densitometry, normalized as described in Methods, and fold induction over orthologous spots in mock (DMEM) treatment indicated (D). Significant fold induction (>2.0) of MHV68/IL6 over WT MHV-68 specified.

Preprints (www.preprints.org) | NOT PEER-REVIEWED | Posted: 3 September 2018 doi:10.20944/preprints201809.0008.v1



*3.3. Functions of proteins induced by MHV-68 in lungs*

While this survey is not a comprehensive list of BAL proteins [34,53], proteins identified fell into four broad functional groups according to Gene Ontology (GO) classification and the scientific literature (Table 1): (i) acute phase response (APR) and inflammation, (ii) oxidative stress response, (iii) phospholipid metabolism and signaling, and (iv) molecular transport and serum proteins. Most of these proteins have been implicated in inflammation or lung diseases, and many have been identified in proteomics studies of BAL from human patients with ARDS [35,36,54], acute lung diseases [33], IPF [37], or proteomics analysis of serum from patients with severe acute respiratory syndrome (SARS) caused by SARS-coronavirus [55]. MHV68/IL6 virus induced three antioxidant (thioredoxin-like 4B, peroxiredoxin 2, superoxide dismutase 3) and two acute phase ( 2-macroglobulin, CRABP2) proteins substantially more than WT MHV-68. Accordingly, oxidative stress [56,57] and acute phase responses [58,59] have been shown to be regulated by IL6.

**Table 1.** Functions of bronchoalveolar lavage proteins identified in MHV-68 infection.

| Spot | BAL Protein Identification | Symbol | GO:terms | GO Functions | Lung Disease Finding |
|---|---|---|---|---|---|
| **Acute Phase Resp./Inflammation** | | | | | |
| 1 | a1-acid glycoprotein 1B | A1AG1 | 0002682 | lipocalin-like immune regulator | APR;TB;IAV |
| 2 | a1-anti-trypsin (serpin A1) | A1AT6 | 0004867 | serine-type endopeptidase inhibitor | APR;ARDS;COPD;SARS;IAV |
| 3 | a2-macroglobulin | A2MP | 0004867 | serum-type endopeptidase inhibitor | APR;ARDS;IPF |
| 11 | Haptoglobin | Hp | 0004252 | serine-type endopeptidase | APR;SARS |
| 12 | IL1 family member 10 | IL1f10 | 0005152 | IL1-receptor antagonist | APR;IPF |
| **Oxidative Stress Response** | | | | | |
| 19 | Superoxide dismutase 3 [Cu-Zn], ex. | EC-SOD | 0006979 | response to oxidative stress | ARDS;NFkB; antioxidant |
| 10 | Glutathione-S-transferase, mu1 | GSTm1 | 0004364 | response to oxidative stress | antioxidant |
| 14 | Peroxiredoxin 2 | Pdx2 | 0006979 | response to oxidative stress | ARDS;SARS;IAV;antioxidant |
| 15 | Peroxiredoxin 6 | Pdx6 | 0000302 | response to reactive oxygen species | Sf-PhL;IAV;antioxidant |
| 20 | Thioredoxin-like 4B | TXNL4B | 0030612 | thioredoxin activity | antioxidant |
| **Phospholipid Metabol./Signaling** | | | | | |
| 8 | Calcyclin | S100a6 | 0048146 | fibroblast proliferation | growth factor |
| 9 | Clara cell protein 10 | CC10 | 0019834 | phospholipase A2 inhibitor | Sf-PhL |
| 13 | Oxytocin receptor | OxtR | 0004990 | oxytocin receptor activity | |
| 16 | Phospholipase A2, secreted | PLA2G12A | 0004623 | phospholipase A2 activity | SARS;IAV;Sf-PhL |
| **Molecular Transport/Serum** | | | | | |
| 5 | Albumin | Alb | 0006810 | molecular transport in serum | |
| 6 | Annexin A5 | Anxa5 | 0050819 | negative regulation of coagulation | anticoagulant |
| 4 | a2-u-globulin (mj urinary protein 6) | Mup6 | 0005550 | lipocalin-like pheromone transport | allergen |
| 7 | Apolipoprotein E | ApoE | 0017127 | cholesterol, lipid transport in | Sf-PhL |
| 17 | Plasma retinol binding protein | RBP4 | 0001972 | plasma retinol & vitamin A carrier | SARS;VA;APR(negative) |
| 18 | Retinoic acid binding protein 2 | CRABP2 | 0001972 | retinoic acid (retinol) binding | APR;VA |
| 22 | Transthyretin | TTR | 0005179 | vitamin A & T4/thyroxine transport | APR;VA |

*3.4. Functional enrichment analysis*

To gain a more systematic understanding of protein functions induced in response to MHV-68 infection of the lung, we undertook bioinformatics analyses to identify functional enrichment for the 20 of 23 significant or marginally significant proteins identified in MHV-68 BAL. Albumin, a reference serum protein, and protein fragments (Hydin and OxtR) were not included. Among BAL proteins, significantly enriched functional categories included physiological stress ($p$=0.0010), oxidative stress annotations ($p$<0.0001), and acute phase response ($p$=0.0028) (Figure 3). Oxidative stress response proteins included reactive oxygen species (ROS) detoxifying enzymes (peroxiredoxins, thioredoxins, and superoxide dismutase). Acute phase response (APR) proteins overlapped with other enriched functions, including physiological stress response and signaling ($p$=0.039). Among signaling proteins, vitamin A (retinoic acid) binding was a significant function ($p$=0.0094) for three proteins that were also induced in APR: CRABP2, transthyretin (TTR), and plasma retinol binding protein (RBP4). Proteins induced by WT MHV-68 infection were predominantly in stress response, acute phase, signaling, and oxidative stress categories. Exogenous expression of IL6 in the context of MHV-68 infection primarily induced oxidative stress and APR proteins as well as vitamin A binding protein CRABP2; RBP4 was weakly induced in the context of IL6. Finally, signaling and APR proteins (calcyclin, Clara cell protein 10, and haptoglobin) were found to be less abundant in WT MHV-68 *v.* control ("suppressed by MHV68", Figure 3) but clearly not oxidative stress proteins.

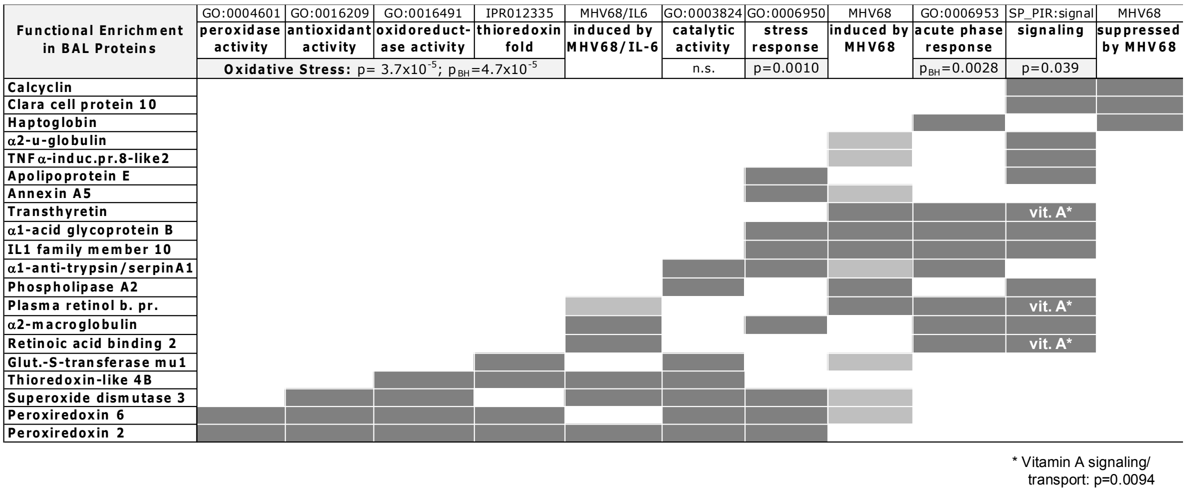


**Figure 3.** Functional enrichment matrix for identified BAL proteins. Protein functional enrichment for 20/23 BAL proteins identified, clustered by Gene Ontology (GO), InterPro (IPR), and Protein Information Resource (SP_PIR) term annotation, Ingenuity Pathways Analysis (IPA), or regulation by WT MHV-68 (MHV68) and MHV68/IL6 (infex). Dark gray, inclusion in functional term or strong regulation. Light gray, weak induction by MHV-68 or MHV68/IL6. Proteins involved in vitamin A (vit. A*) signaling and transport were enriched within the signaling category with $p$=0.0094. $p$-values for enrichment in annotated functional categories; Benjamini-Hochberg $p_{BH}$ false discovery probability values for IPA category analysis.

*3.5. Acute phase and oxidative stress gene expression in the MHV-68 infected lung*

To further investigate acute phase and oxidative stress responses in lung tissue, the expression of known host genes involved in these pathways was studied by quantitative real-time (qRT) PCR. Mice were infected with WT MHV-68, MHV68/IL6, or mock (DMEM) inoculated, and RNA was extracted from total lung homogenates for qRT-PCR. By 7d.p.i., APR/vitamin A transport genes RBP4 and TTR were upregulated approximately 4- and 2-fold, respectively, with significantly higher induction by MHV68/IL6 for RBP4 (Figure 4). MHV-68 infection also generally induces oxidative stress genes in the lung by 7d.p.i. (Figure 4), including genes encoding lung antioxidant

Preprints (www.preprints.org) | NOT PEER-REVIEWED | Posted: 3 September 2018 doi:10.20944/preprints201809.0008.v1



proteins Pdx6, EC-SOD, glutathione peroxidase 3 (Gpx3), and thioredoxin 1 (Trx1), as well as inducible nitric oxide synthetase (iNOS), a pro-inflammatory protein that is capable of generating reactive oxygen species (ROS) and reactive nitrogen species (RNS) as a byproduct of the production of NO messenger [61].

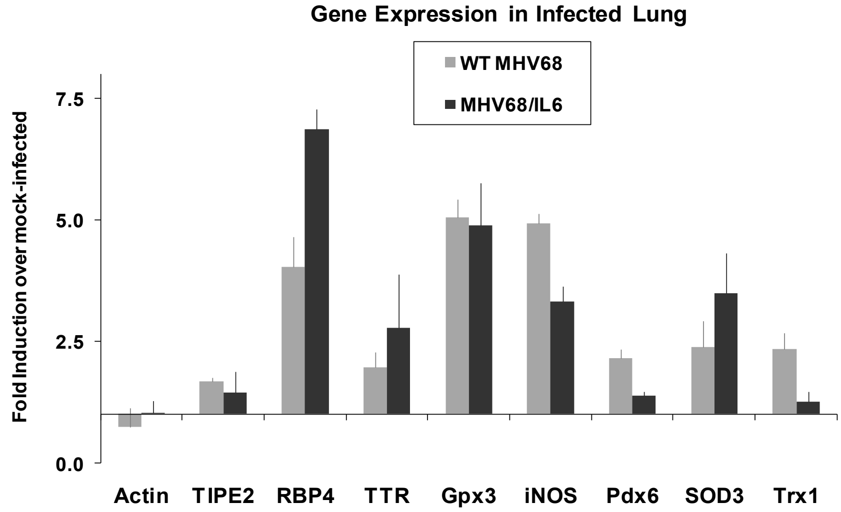


| | Actin | TIPE2 | RBP4 | TTR | Gpx3 | iNOS | Pdx6 | SOD3 | Trx1 |
|---|---|---|---|---|---|---|---|---|---|
| WT v. Mock | n.s. | * | *** | ** | *** | *** | *** | ** | *** |
| IL6 v. Mock | n.s. | n.s. | *** | * | *** | *** | n.s. | ** | n.s. |
| WT v. IL6 | n.s. | n.s. | *** | n.s. | n.s. | *** | *** | n.s. | ** |

**Figure 4.** MHV-68 infection upregulates stress-response genes in the lungs of infected mice. Mice were mock-infected, or infected i.n. with $2x10^5$ pfu of WT MHV-68 or MHV68/IL6. Total lung RNA was isolated 7 d.p.i., and qRT-PCR performed with specific primers to murine acute phase, immunomodulatory, oxidative stress response genes, and actin. *p*-values of fold induction estimated from unpaired, 2-tailed t-test (sub-table) with p<0.01 (***), p<0.05 (**), p<0.1 (*), or p>0.1 (n.s., not significant). *TIPE2*, Tnfaip8l2; *Gpx3*, glutathione peroxidase 3; *iNOS*, inducible nitric oxide synthetase; *SOD3*, (extracellular) superoxide dismutase 3; *Trx1*, thioredoxin 1; *RBP4*, *TTR*, *Pdx6*, as in Table S2.

*3.6. Lytic MHV-68 infection induces oxidative stress in cultured fibroblasts*

To investigate the autonomous contribution of the MHV-68 lytic phase to oxidative stress in infected cells, we studied the role of MHV-68 lytic phase in the production of ROS in murine NIH3T3 fibroblasts and human lung epitheloid A549 cells. As a control, we treated uninfected NIH3T3 cells with hydrogen peroxide, and induction of ROS was evident by oxidative green fluorescence of $H_2DF_2DA$ (Figure 5A, upper panel). To examine whether ROS is induced by MHV-68 infection, subconfluent NIH3T3 or A549 cells were infected with a recombinant MHV-68 virus expressing red fluorescent protein (RFP) from the ORF28 late locus, and then stained with $H_2DF_2DA$ at 20 hours post-infection (h.p.i). The majority of infected NIH3T3 or A549 cells (indicated by red fluorescence) exhibited a moderate to bright green $H_2DF_2DA$ oxidative fluorescence, indicative of a high level of ROS (Figure 5A, lower two panels). Roughly 15% of infected NIH3T3 exhibited bright $H_2DF_2DA$ oxidative fluorescence, indicative of a high level of ROS, by 20h.p.i. (Figure 5A). ROS can lead to the generation of peroxides such as $H_2O_2$, which are reduced by the multi-subunit catalase enzyme.

Indeed, catalase enzyme (Figure 5B) and catalase activity (Figure 5C) were upregulated in NIH3T3 cells infected with WT MHV-68 (m.o.i.=1) by 24h.p.i. In contrast, only basal catalase activity was observed early during MHV-68 infection at 2h.p.i. and 6h.p.i, analogous to simply adding excess $H_2O_2$ (Figure 5C). ROS did not accumulate by 4h.p.i. even in a high titer infection (m.o.i.=5), but did by 20h p.i. (Figure S3), suggesting that cytotoxicity associated with the late lytic cycle of virus infection is required for generation of ROS. However, ROS induction itself seems to have little effect on MHV-68 infection; modulating cellular redox potential in infected NIH3T3 cells with sublethal doses of the oxidative stress inducer paraquat only weakly enhanced lytic expression of RFP/MHV-68, and quenching ROS with soluble glutathione had little discernable effect (Figure S3).

**Fig. 5**

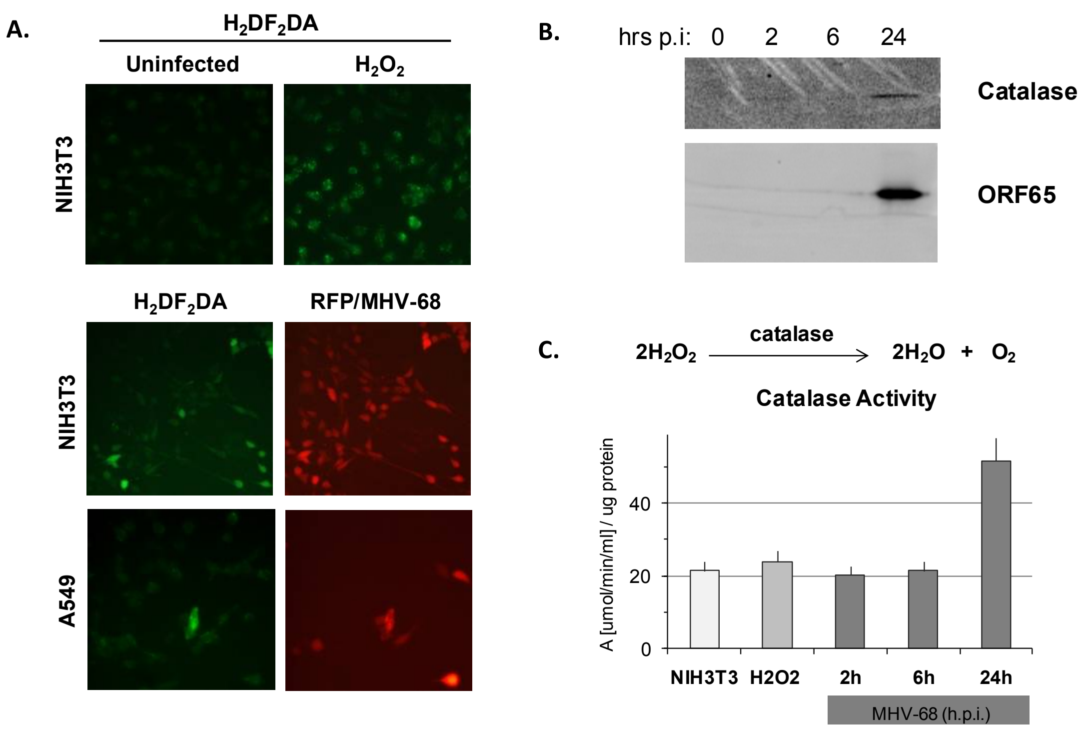


**Figure 5.** MHV-68 infection induces reactive oxygen species (ROS) in cultured cells. **(a)** Murine NIH3T3 fibroblasts or human lung A549 cells were infected (m.o.i.=1) with MHV-68 expressing red fluorescent protein (RFP/MHV-68, *red channel*). Supernatants were removed 20 h.p.i., cells incubated with $H_2DF_2DA$, and imaged by epifluorescence microscopy. Hydrogen peroxide ($H_2O_2$) was a control for induction of ROS leading to oxidative fluorescence of $H_2DF_2DA$ *(green channel)*. **(b)** NIH3T3 cells infected with WT MHV-68 were lysed at the indicated times, proteins separated by SDS-PAGE, and Western blots probed for catalase protein and MHV-68 lytic antigen (ORF65) with specific antibodies and electrochemiluminescent secondary antibody detection. **(c)** Induction of ROS measured by catalase activity assay. NIH3T3 cells were untreated, treated with $H_2O_2$ for 20h, or infected with WT MHV-68 for the times indicated; cells were lysed and aliquots measured for protein content by Bradford and catalase activity according to a standard curve.

*3.7. An oxidative stress response network induced in the mouse lungs by MHV-68 infection*

To gain a deeper understanding of the pathways induced in response to MHV-68 infection of the lung and co-expression of IL6, we used Ingenuity Pathways Analysis (IPA) to extract an oxidative stress and inflammatory response network centered on redox proteins identified in this study. While the number of proteins identified in our proteomics study (Table S1) was insufficient for *de novo* network discovery [62], analog curation using data from the Ingenuity KnowledgeBase and NCBI EntrezGene allowed synthesis of a model depicting regulatory interactions (*i.e.*, activation, inhibition, *etc.*) among key molecules (Figure 6). A striking feature of the model is the multi-directional interaction between antioxidant proteins and transcriptional regulatory factors such as COX-2, NF B, and iNOS, all of which have been found to be important to gammaherpesvirus infections [25,63,64].

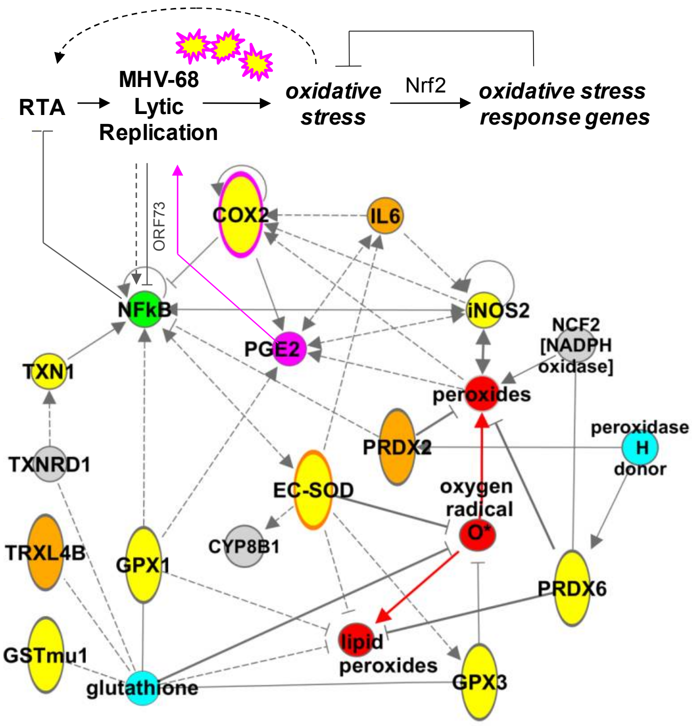


**Figure 6.** Oxidative stress network induced in the mouse lungs by MHV-68. A sub-network of antioxidant proteins was extracted by IPA and manually curated. MHV-68 lytic infection induces reactive oxygen species (ROS) small molecules *(red)* that in turn induce oxidative stress response genes. Network model includes proteins induced in infected lungs by MHV-68 *(yellow)* or by IL6 in the context of MHV-68 infection (*orange* and *orange-border*), proteins directly upregulated by MHV-68 lytic infection (*pink* and *pink-border*, ref. [64]), and NF B, which has a complex interaction with MHV-68 lytic replication (*green*, ref. [63]). Antioxidant co-factors *(aqua)*; other redox proteins *(gray)*; activating interactions *(arrows)*, indirect regulation *(dashed arrows and bars)*, and inhibitory interactions *(blocking bars)* indicate potential complexity of even a small-scale redox network *in vivo*.

## 4. Discussion

We have undertaken a differential proteomics analysis of BAL fluid to gain insight into the pulmonary molecular pathology of respiratory virus infections in the mouse. As a tractable animal model of gammaherpesvirus infection, the pathogenesis and immune response to MHV-68 in the mouse lung has been a subject of considerable recent inquiry [16,18-21,23,49,65]. In such studies, BAL

Preprints (www.preprints.org) | NOT PEER-REVIEWED | Posted: 3 September 2018 doi:10.20944/preprints201809.0008.v1



fluid has been used to analyze immune cell infiltration, cytokine/chemokines profiles, and chemotaxis activity, for example [15,20]. We found molecules in BAL fluid that provide additional insight as virus-induced lung injury is resolved, uncovering molecular details (*i.e.*, host factors and pathways) of host response to a virus in a quantifiable manner. Proteins induced by 9d.p.i. included oxidative stress response proteins, acute phase proteins, signaling molecules and transporters (Table 1). Functional category analyses indicated that redox, acute phase, and vitamin A proteins were significantly enriched in the subset of BAL proteins we identified (Figure 3), suggesting that these processes are induced by 9d.p.i. in MHV-68 infection of the mouse lung.

### *4.1. Effects of co-expressing IL6*

As suggested by experiments in IL6-deficient mice [30], IL6 may play a role in inflammation and the development of lung pathology during MHV-68 infection rather than impacting viral replication. Instead of comparing BAL proteins between WT and IL6-deficient mice, we took a different approach to examine the effects of IL-6 by using an MHV68/IL6 virus that over-expresses this cytokine. Co-expression of IL6 in MHV-68 infection of the mouse lung showed neither significant difference in replication kinetics nor whole lung viral titers in comparison to wild-type virus (data not shown). However, MHV68/IL6 induced a subset of BAL proteins, including redox, acute phase, and vitamin A signaling/transport molecules (Figure 2D), as well as type I collagen (Figure 1B). IL6 gene expression is induced by NF B heterodimers, and IL6 in turn signals through an IL6 (CD126) receptor-gp130 co-receptor complex on a subset of B-cells to NF-IL6, a pro-inflammatory transcription factor [66,67]. In the lung, IL6 regulates natural killer (NK) cells responding to MHV-68 infection [30]. KSHV, a human gammaherpesvirus, encodes a viral IL6 homologue that can signal though the gp130 co-receptor found on a range of B-cells, independently of the cellular IL6 receptor [68]. The KSHV lytic transactivator RTA also activates the human IL6 promoter [69]. In addition, KSHV microRNAs (miRNA) specifically induce IL6 and IL10 in macrophages [70]. Besides querying the effects of supranormal IL6 levels on infected lung pathophysiology, inclusion of the MHV68/IL6 virus in our BAL proteomics analysis allowed development of an analytical IEF/2DE method for differential protein discovery (Figure 2), demonstrating the potential utility of this approach for querying viral mutants.

### *4.2. Oxidative stress response proteins are induced in MHV-68 infection of the mouse lung*

In the BAL proteome, host antioxidant and oxidative stress response proteins were upregulated by MHV-68 infection (Table 1), including Pdx6, EC-SOD, and a paralogue of GST (GSTm1). In whole lung tissue, genes encoding iNOS, extracellular glutathione peroxidase (Gpx3), and a thioredoxin (Trx1), were also induced (Figure 4). Co-expression of IL6 in MHV-68 infection further upregulated EC-SOD (Figure 2D), and induced another peroxiredoxin (Pdx2) and a thioredoxin paralogue (TXNL4B). Induction of antioxidant proteins suggests a pathophysiological response in the lungs to oxidative stress. Induction of oxidative stress has been found in experimental virus infections *in vivo*, including RSV in mice [43,71], and influenza virus infections in human epithelial cells, mice [72,73] and macaques [74]. Antioxidant proteins can protect lung tissue from oxidative damage, detoxify oxidized phospholipids, and reduce virus-associated ALI [73,75,76]. Oxidative stress induced in respiratory virus infections can also have pleiotropic effects on lung gene expression and inflammatory processes such as cytokine and chemokine production [72,74,77].

 doi:10.20944/preprints201809.0008.v1



*Sources of oxidative stress.* We found that MHV-68 infection of cultured NIH3T3 fibroblasts or lung-derived A549 cells induces ROS and catalase activity (Figure 5). Similarly, cultured cells infected with respiratory syncytial virus (RSV), rhesus monkey rhadinovirus (RRV, another gammaherpesvirus), or HSV-1 show increased oxidative stress [43,78-80]. Two genes upregulated by MHV-68, COX-2 [64] and iNOS (Figure 4), are capable of directly generating ROS as reaction byproducts [61,81]. Lytic MHV-68 infection proceeds under conditions of oxidative stress, as we found that treating infected cells with paraquat did not inhibit but rather mildly enhanced RFP/MHV-68 virus infection (Figure S3). *In vivo*, mice treated with NSAID targeting COX-2 showed no differences in MHV-68 titers than controls [[64] and unpublished data]. In contrast, cytotoxic T-lymphocyte (CTL) immune control of MHV-68 is impaired in mice deficient in iNOS, resulting in lethality [25]. While viral infection of type I and II lung epithelial cells likely contributes directly to the induction of oxidative stress, there may be other contributing factors in the alveolar microenvironment, such as degranulation of activated innate immune effector cells (alveolar macrophages, natural killer cells, and neutrophils). For example, the Ncf1/NADPH oxidase complex in neutrophils also significantly contributes to ROS and oxidation of phospholipids in lung insulted with H5N1 highly pathogenic avian influenza (HPAI) [56].

*Oxidative damage to surfactant phospholipids.* Pulmonary surfactant lipids and proteins have roles in antiviral defense, inflammatory and immune responses against respiratory viruses such as influenza A viruses, RSV, and adenovirus [82]. Conversely, oxidative damage to phospholipids is implicated in ALI caused by viruses such as HPAI, SARS-CoV [56], and RSV [71]. Oxidized phospholipids that accumulate in HPAI and SARS-CoV infections also likely contribute to ALI and hypercytokinemia ("cytokine storm") by signaling though Toll-like receptor 4 (TLR4) and TRIF in macrophages, activating NF B and inducing IL6 [56]. We found PLA2G12A, a secreted phospholipase A2 enzyme, highly upregulated in BAL from MHV-68 infected mice at 9d.p.i. (Table 1 and Figure 2D). Phospholipase A2 enzymes are involved in the degradation of damaged (oxidized) surfactant phospholipids including dipalmitoyl phosphatidylcholine (DPPC), a process often upregulated in lung injury. Phospholipase A2 is inhibited by abundant surfactant proteins including surfactant protein A (SP-A; [83]), and Clara cell protein 10 (CC10), which was downregulated in BAL from MHV-68 infection (Figure 2D). Another protein induced in BAL, Pdx6, may reduce oxidized phospholipids, including DPPC, that have been modified by ROS, allowing lipid recycling in type II epithelial cells or macrophages in the lungs [84-86]. Accordingly, surfactant protein expression is altered in chronic MHV-68 infection of IFNGR-null mice that display a pathology reminiscent of IPF [15]. These finding suggest a role for lung surfactant lipids and lipid-associated proteins in the pathogenesis of MHV-68 in the lungs.

*Comparison to other respiratory diseases and role of Nrf2.* In contrast to MHV-68 infection, expression of antioxidant (oxidative stress response) proteins SOD1, GPx1, Pdx6, GSTmu1, and catalase were suppressed during RSV infection in the lungs of mice and human patients [43]. The antioxidant transcription factor Nrf2 was also suppressed in RSV infection, while Pdx2 was induced like in MHV-68 infection. The importance of Nrf2-mediated response was illustrated in knockout mice, whereby Nrf2 protected lung cells from bronchopulmonary injury by RSV and influenza A virus [71,72]. Interestingly, a close association between oxidative stress and pro-fibrotic inflammation in the lung, marked by elevated Nrf2 expression, is well-established in human patients with IPF and/or interstitial pneumonia [87,88]. Human Pdx2 particularly has also been found upregulated in UIP/IPF lung tissue,

Preprints (www.preprints.org) | NOT PEER-REVIEWED | Posted: 3 September 2018 doi:10.20944/preprints201809.0008.v1



in particularly in alveolar macrophages [89]. Thus, the role of Nrf2 in the induction of antioxidant defenses and pro-fibrotic pathophysiology of MHV-68 is under further investigation.

*4.3. Modeling a complex relationship*

A network of molecules intersect with these antioxidant proteins, including NF B, IL6, COX-2, iNOS, Nrf2, and small molecules, suggesting multiple points at which MHV-68 infection might generate an oxidative stress in the lungs (Figure 6). For example, while it is suspected that NF B can be activated by oxidative stress in viral infections [71,72], the relationship between NF B signaling and gammaherpesvirus pathogenesis is complex and poorly understood. It has been reported that NF B is activated by MHV-68 lytic replication [48], while paradoxically, NF B activation can also inhibit the initiation of MHV-68 lytic replication [63]. Regulation of NF B is an enriched function among cellular proteins interacting with MHV-68 proteins [90], and the lytic protein ORF73 promotes ubiquitination and degradation of p65/RelA [91]. Likewise, inhibition of NF B leads to upregulation of ROS and reactivation of latent KSHV by activating expression of the lytic transactivator protein, RTA [92]. Moreover, experimental inhibition of NF B blocks chemokine responses and development of pulmonary fibrosis in the lung in MHV-68 infection [48]. Functional genomics studies may provide additional molecular insight into virus-host interactions controlling MHV-68 infection and induction of oxidative stress [90].

*Acute phase response.* appearance of acute phase proteins in the serum is a hallmark of systemic inflammation resulting from infections, including bacterial sepsis, pneumonia, and human immunodeficiency virus (HIV-1) [93-96]. The release of acute phase proteins from liver hepatocytes or other tissues is dependent on IL6 and other cytokines [97,98]. The finding of acute phase proteins in BAL from MHV-68 infected mice indicate a systemic response to intranasal MHV-68 infection, or leakage of serum proteins into the pleural interstitial and alveolar lumen, consistent with previous findings of UIP pathology in MHV-68 infection [16]. We found acute phase-related proteins in BAL at 9d.p.i, including 1-antitrypsin (A1AT6), 2-macroglobulin (A2MP), 1-acid glycoprotein 1B (A1AG1/AGP), haptoglobin, and vitamin A transport molecules CRABP2, TTR, and RBP4 (Table 1 and Figure 3). AGP is immunomodulatory, induced in experimental pulmonary tuberculosis [99] and influenza [58] in mice. A1AT6 is a protease inhibitor induced by MHV-68, while the endopeptidase haptoglobin is suppressed (Figure 2D); along with type I collagen accumulation (Figure 1B), an anti-proeolytic lung tissue remodeling environment is apparent. IL6 has also been suggested to enhance the production of acute phase response proteins in virus infections [97]. Indeed, the protease inhibitor A2MP is induced in MHV68/IL6 infection (Figure 2D), consistent with higher type I collagen deposition. Finally, vitamin A (retinoic acid, RA) is a signaling molecule carried in the serum as all-trans retinol by an RBP4 and TTR dimer complex [100]. Vitamin A inhibits HSV-1 [101] and KSHV [102] replication in cell culture. Vitamin A can activate immune response to infection in the respiratory tract, for example, by enhancing Th2 responses and IgA secretion in influenza virus infection of mice [103]. In the lungs, vitamin A counter-acts IL6 and protects against bleomycin-induced fibrotic lung injury [104,105]. The immunoregulatory function of vitamin A is not understood in MHV-68 infection.

*Other immunomodulatory proteins in BAL fluid.* One gene encoding an immune modulator, Tnfaip8l2, was induced in BAL by MHV-68 infection by 9d.p.i. (Table 2). While LC/MS-MS peptide data identifying this protein was of marginal significance (p<0.1), the gene encoding Tnfaip8l2 was

 doi:10.20944/preprints201809.0008.v1



also weakly upregulated in lung tissue by 7d.p.i. (Figure 4). TNF -interacting protein 8 members, including Tnfaip8l2 (TIPE2), form a conserved gene family in humans and mice (Figure S4) involved in immune homeostasis. TIPE2 downregulates inflammatory responses mediated by Toll-like receptor (TLR), T cell receptor (TCR), and NFκB signaling, which in turn promotes Fas-mediated apoptosis in lymphoid cells [106]. Except for Tnfaip8l2 and a weak match to annexin A5, we did not find other cell death regulators in BAL at 9 d.p.i.. Cell death in MHV-68 infection has been found to be mediated by CD8+ CTL in the lung [23], while a viral Bcl2 encoded in the MHV-68 genome blocks internal cell death mechanisms such as autophagy in infected cells [107].

### *4.4. Limitations of this study*

Our BAL processing protocol enriched for differentially-expressed proteins remaining after reduction of abundant high-MW macromolecules, including albumin, immunoglobulins, and serum proteins (Figure 1C). While this approach allowed us to resolve less-abundant proteins, it likely missed potentially interesting proteins associated with removed macromolecules. We also did not detect a high diversity of cytokines in post-processed BAL, possibly because of their relatively low abundances, interactions with antibody or albumin, or failure to isolate highly basic proteins in the purification schema. Variant protocols enriching different BAL fractions, or using different BAL solvents, and new mass spectrometry technologies are in development.

## 5. Conclusions

*Experimental MHV-68 infection of the mouse as a model for lung diseases.* The induction of and responses to oxidative stress appear to be a common theme in the pathophysiology of interstitial lung diseases, including infections such as MHV-68 (this study and [15]), SARS-coronavirus [55], influenza A virus [56,72], RSV [43], and in chronic diseases such as COPD [108] and IPF [87]. Interestingly, a number of the gene products we identified as differentially regulated by MHV-68 infection in BAL were also found associated with these diseases (Table 1). Differential proteomics analysis of mouse BAL fluid opens a new window into understanding the pathogenesis of MHV-68 and other respiratory viruses, and MHV-68 models of chronic lung diseases such as IPF [15]. The proteins identified herein are potential biomarkers for pulmonary virus infections generating high levels of oxidative stress and aggravating other pathophysiological responses, such as acute phase (Figure 3) and surfactant lipid damage. We propose continuing application of differential BAL proteomics in conjunction with whole-lung genomics and proteomics analyses [74,109], to integrate systems understanding of immune responses and virus-induced pathological changes to the pleura.

**Supplementary Materials:** The following are available online at www.mdpi.com/link,

Table S1: Proteomics identification of proteins in murine BAL fluid from MHV-68 infection

Table S2. RT-PCR primers used in this study.

Figure S1. Analysis of viral and cellular components in BAL fluid.

Figure S2. One of the LC/MS-MS spectra identifying mouse Pdx6.

Figure S3. Dynamics of ROS generation in MHV-68 infection of cultured cells.

**Acknowledgments:** We would like to thank Sara Bassilian, Pete Psoudas, James Kerwin, and Kym Faull of the Proteomics Shared Resource at UCLA; Leming Tong, Zhou Zhou, Seungmin Hwang, Xudong Li and Neil Bortz for technical assistance; and Jason Burkhead (UAA) for helpful discussions. This work was supported by a Genomics Seed Grant from the Jonsson Comprehensive Cancer Center at UCLA and NIH (to R.S.); and a pilot award from NIGMS Alaska INBRE P20GM103395 (to E.B.).

 doi:10.20944/preprints201809.0008.v1



**Author Contributions:** E.B., T.-T.W. and R.S. conceived and designed the experiments; E.B. and J.P.W. performed the experiments; E.B., J.P.W., T.-T.W. and R.S. analyzed the data; E.B. wrote the paper.

**Conflicts of Interest:** The authors declare no conflict of interest. The funding sponsors had no role in the design of the study; in the collection, analyses, or interpretation of data; in the writing of the manuscript, and in the decision to publish the results.

**Appendix A.** Supplemental Table and Supplemental Data Figures.

**Table S1.** Proteomics identification of proteins in murine BAL fluid from MHV-68 infection. Proteomics identification of BAL (differentially expressed) proteins from BAL fluid from mock (DMEM), MHV-68 infected, and MHV-IL6 infected mice at 9d. p.i. Proteins spots from 2D-E were excised, digested in trypsin, and identified by MALDI and/or LC/MS-MS. Spots were also quantified by densitometry, normalized as described in Methods, to estimate fold induction over mock (DMEM) control.

**Table S1 Notes:**

[1] UniProt Accession number *(Mus musculus).*

[2] Number of matching peptides in mass spectromtery; range indicated for multiple spots/detections.

[3] Significance of mass spectrometry identification: LC/MS-MS, using Mascot software, listing highest individual peptide M score: M>38, $p$<0.05 (significant); 38>M>23, $p$<0.10 (*marginal significance); or MALDI, using Aldente software, listing Z-score and % peptide sequence coverage; *n.d.*, not detected; *n.s.*, not significant.

[4] Regulation of protein abundance in mouse BAL from WT MHV-68 or MHV68/IL6 at 9d.p.i. estimated by normalized ratio of each protein's total 2D-E spot density to orthologous spot in mock (DMEM) control 2D-E; regulation indicated in key.

**Table S2.** RT-PCR primers used in this study. Source of primer sequences from references specified or RT-PCR primer database listed.

**Figure S1.** Analysis of viral and cellular comnponents in BAL fluid. BAL fluid from uninfected (DMEM-inoculated), WT MHV-68-infected or MHV68/IL6-infected mice was recovered at 6 d.p.i. and 9 d.p.i., pooled, and separated by centrifugation into supernatant and cellular phases. **(a)** Viral DNA copies in BAL fluid supernatant was analyzed by quantitative PCR according to reference standards. **(b)** Proteins in processed BAL fluid supernatant were separated by SDS-PAGE and viral ORF65/M9 capsid protein was detected by Western blot with polyclonal antisera. NIH3T3 cells infected with WT MHV-68 provided a positive control for ORF65/M9 antisera. BAL supernatant Western blot was also probed with monoclonal HRP-labeled goat anti-mouse secondary antibody alone, detecting mouse IgG heavy chain (H.C.) as indicated. **(c)** BAL cells pelleted by low speed centrifugation were resuspended on glass slides and stained by hematoxylin-eosin. BAL cells were predominantly (>75%) mononuclear; erythrocytes *(arrowhead)* and cellular/fibrous debris or platelets *(arrow)* were also occasionally visible.

**Figure S2.** One of the LC/MS-MS spectra identifying mouse Pdx6. Protein spots excised from SYPRO-Ruby stained 2D-PAGE were digested in trypsin, separated by LC, and peptides analyzed on a Sciex Q-star ion trap mass spectrometer with tandem peptide ion fragmentation running in data-

 doi:10.20944/preprints201809.0008.v1



dependent mode. Peptide mass (*Mr* or *m*) and charge (*z*) and MS/MS fragment ions were analyzed by *Mascot* software with error tolerance <1 Da, 1 tryptic digest miss allowed, fixed carbamamidomethyl modification of cysteine, and variable oxidation of methionine. Data were searched against the non-redundant mouse proteome identifying 7 peptides to a database isoform of mouse peroxiredoxin 6 ("Protein View") with composite protein match probability score calculated (match probability, log $p=10^{-\mathrm{SCORE}}$). Fragment ion MS/MS spectra were displayed by *m/z* and intensity and matched to predicted a-, b- and y-series fragmentation ions ("Peptide View"). Additional fragment ion spectra matches with ion expectation scores were considered but are below significance cutoff of 38 ($p<0.05$).

**Figure S3.** ROS during MHV-68 infection in cultured fibroblasts. **(a)** MHV-68 does not induce ROS by 4 h.p.i. Murine NIH3T3 fibroblasts were infected (m.o.i.=5) with RFP/MHV-68 (*red channel*). Supernatants were removed at 4 or 20 h.p.i., replaced with PBS containing $H_2DF_2DA$, and cells imaged by epifluorescence microscopy. Paraquat (10uM) was a control for induction of ROS leading to oxidative fluorescence of $H_2DF_2DA$ *(green channel)*. **(b)** Modulation of ROS does not drastically affect MHV-68 replication. Untreated NIH3T3 cells or cells treated with soluble glutathione (GSH), a ROS quencher, or increasing concentrations of paraquat, a ROS inducer, were infected with RFP/MHV-68 (m.o.i.=1) and imaged 20 h.p.i.

**Figure S4.** Tnfaip8l2 is a member of a conserved gene family in human and mouse. Amino acid sequences for human and murine homologues of TNF -induced protein 8 were retrieved by UniProt database Accessions and aligned by CLUSTAL. TP8L2_mouse is Tnfaip8l2, also called mouse TIPE2, the protein identified in this study. Similarity indicated for conserved residues (!), similar residues (:), and weakly similar residues (.).

## References

1. Belser JA, Maines TR, Tumpey TM, Katz JM (2010) Influenza A virus transmission: contributing factors and clinical implications. Expert Rev Mol Med 12: e39.
2. do Carmo Debur M, Raboni SM, Flizikowski FB, Chong DC, Persicote AP, et al. (2010) Immunohistochemical assessment of respiratory viruses in necropsy samples from lethal non-pandemic seasonal respiratory infections. J Clin Pathol 63: 930-934.
3. Gao R, Dong L, Dong J, Wen L, Zhang Y, et al. (2010) A systematic molecular pathology study of a laboratory confirmed H5N1 human case. PLoS One 5: e13315.
4. Kaye M, Skidmore S, Osman H, Weinbren M, Warren R (2006) Surveillance of respiratory virus infections in adult hospital admissions using rapid methods. Epidemiol Infect 134: 792-798.
5. Ksiazek TG, Erdman D, Goldsmith CS, Zaki SR, Peret T, et al. (2003) A novel coronavirus associated with severe acute respiratory syndrome. N Engl J Med 348: 1953-1966.
6. Papenburg J, Boivin G (2010) The distinguishing features of human metapneumovirus and respiratory syncytial virus. Rev Med Virol 20: 245-260.
7. Quan PL, Palacios G, Jabado OJ, Conlan S, Hirschberg DL, et al. (2007) Detection of respiratory viruses and subtype identification of influenza A viruses by GreeneChipResp oligonucleotide microarray. J Clin Microbiol 45: 2359-2364.

Preprints (www.preprints.org) | NOT PEER-REVIEWED | Posted: 3 September 2018 doi:10.20944/preprints201809.0008.v1



8. Estenssoro E, Rios FG, Apezteguia C, Reina R, Neira J, et al. Pandemic 2009 influenza A in Argentina: a study of 337 patients on mechanical ventilation. Am J Respir Crit Care Med 182: 41-48.

9. Koegelenberg CF, Irusen EM, Cooper R, Diacon AH, Taljaard JJ, et al. (2010) High mortality from respiratory failure secondary to swine-origin influenza A (H1N1) in South Africa. QJM 103: 319-325.

10. Mohan A, Chandra S, Agarwal D, Guleria R, Broor S, et al. Prevalence of viral infection detected by PCR and RT-PCR in patients with acute exacerbation of COPD: a systematic review. Respirology 15: 536-542.

11. Satterwhite L, Mehta A, Martin GS Novel findings from the second wave of adult pH1N1 in the United States. Crit Care Med 38: 2059-2061.

12. Bhoopat L, Rangkakulnuwat S, Okonogi R, Wannasai K, Bhoopat T (2010) Cell reservoirs of the Epstein-Barr virus in biopsy-proven lymphocytic interstitial pneumonitis in HIV-1 subtype E infected children: identification by combined in situ hybridization and immunohistochemistry. Appl Immunohistochem Mol Morphol 18: 212-218.

13. Saito F, Ito T, Connett JM, et al. (2013) MHV68 latency modulates the host immune response to influenza A virus. Inflammation: 36(6):1295-1303.

14. Muller A, Franzen C, Klussmann P, Wagner M, Diehl V, et al. (2000) Human herpesvirus type 8 in HIV-infected patients with interstitial pneumonitis. J Infect 40: 242-247.

15. Mora AL, Torres-Gonzalez E, Rojas M, Xu J, Ritzenthaler J, et al. (2007) Control of virus reactivation arrests pulmonary herpesvirus-induced fibrosis in IFN-gamma receptor-deficient mice. Am J Respir Crit Care Med 175: 1139-1150.

16. Hughes DJ, Kipar A, Sample JT, Stewart JP (2010) Pathogenesis of a model gammaherpesvirus in a natural host. J Virol 84: 3949-3961.

17. Weslow-Schmidt JL, Jewell NA, Mertz SE, Simas JP, Durbin JE, et al. (2007) Type I interferon inhibition and dendritic cell activation during gammaherpesvirus respiratory infection. J Virol 81: 9778-9789.

18. Lee KS, Cool CD, van Dyk LF (2009) Murine gammaherpesvirus 68 infection of gamma interferon-deficient mice on a BALB/c background results in acute lethal pneumonia that is dependent on specific viral genes. J Virol 83: 11397-11401.

19. Sarawar SR, Cardin RD, Brooks JW, Mehrpooya M, Hamilton-Easton AM, et al. (1997) Gamma interferon is not essential for recovery from acute infection with murine gammaherpesvirus 68. J Virol 71: 3916-3921.

20. Sarawar SR, Lee BJ, Anderson M, Teng YC, Zuberi R, et al. (2002) Chemokine induction and leukocyte trafficking to the lungs during murine gammaherpesvirus 68 (MHV-68) infection. Virology 293: 54-62.

21. Sarawar SR, Cardin RD, Brooks JW, Mehrpooya M, Tripp RA, et al. (1996) Cytokine production in the immune response to murine gammaherpesvirus 68. J Virol 70: 3264-3268.

22. Dutia BM, Allen DJ, Dyson H, Nash AA (1999) Type I interferons and IRF-1 play a critical role in the control of a gammaherpesvirus infection. Virology 261: 173-179.

23. Ehtisham S, Sunil-Chandra NP, Nash AA (1993) Pathogenesis of murine gammaherpesvirus infection in mice deficient in CD4 and CD8 T cells. J Virol 67: 5247-5252.

 doi:10.20944/preprints201809.0008.v1




24. Fuse S, Obar JJ, Bellfy S, Leung EK, Zhang W, et al. (2006) CD80 and CD86 control antiviral CD8+ T-cell function and immune surveillance of murine gammaherpesvirus 68. J Virol 80: 9159-9170.
25. Kulkarni AB, Holmes KL, Fredrickson TN, Hartley JW, Morse HC, 3rd (1997) Characteristics of a murine gammaherpesvirus infection immunocompromised mice. In Vivo 11: 281-291.
26. Dias P, Shea AL, Inglis C, Giannoni F, Lee LN, et al. (2008) Primary clearance of murine gammaherpesvirus 68 by PKCtheta-/- CD8 T cells is compromised in the absence of help from CD4 T cells. J Virol 82: 11970-11975.
27. McMillan TR, Moore BB, Weinberg JB, Vannella KM, Fields WB, et al. (2008) Exacerbation of established pulmonary fibrosis in a murine model by gammaherpesvirus. Am J Respir Crit Care Med 177: 771-780.
28. Lin WC, Lin CF, Chen CL, Chen CW, Lin YS (2010) Prediction of outcome in patients with acute respiratory distress syndrome by bronchoalveolar lavage inflammatory mediators. Exp Biol Med (Maywood) 235: 57-65.
29. Xie XH, Law HK, Wang LJ, Li X, Yang XQ, et al. (2009) Lipopolysaccharide induces IL-6 production in respiratory syncytial virus-infected airway epithelial cells through the toll-like receptor 4 signaling pathway. Pediatr Res 65: 156-162.
30. Sarawar SR, Brooks JW, Cardin RD, Mehrpooya M, Doherty PC (1998) Pathogenesis of murine gammaherpesvirus-68 infection in interleukin-6-deficient mice. Virology 249: 359-366.
31. Chatterjee M, Osborne J, Bestetti G, Chang Y, Moore PS (2002) Viral IL-6-induced cell proliferation and immune evasion of interferon activity. Science 298: 1432-1435.
32. Hu F, Nicholas J (2006) Signal transduction by human herpesvirus 8 viral interleukin-6 (vIL-6) is modulated by the nonsignaling gp80 subunit of the IL-6 receptor complex and is distinct from signaling induced by human IL-6. J Virol 80: 10874-10878.
33. Gharib SA, Nguyen E, Altemeier WA, Shaffer SA, Doneanu CE, et al. (2009) Of mice and men: comparative proteomics of bronchoalveolar fluid. Eur Respir J 35: 1388-1395.
34. Wattiez R, Falmagne P (2005) Proteomics of bronchoalveolar lavage fluid. J Chromatogr B Analyt Technol Biomed Life Sci 815: 169-178.
35. de Torre C, Ying SX, Munson PJ, Meduri GU, Suffredini AF (2006) Proteomic analysis of inflammatory biomarkers in bronchoalveolar lavage. Proteomics 6: 3949-3957.
36. Schnapp LM, Donohoe S, Chen J, Sunde DA, Kelly PM, et al. (2006) Mining the acute respiratory distress syndrome proteome: identification of the insulin-like growth factor (IGF)/IGF-binding protein-3 pathway in acute lung injury. Am J Pathol 169: 86-95.
37. Rottoli P, Magi B, Perari MG, Liberatori S, Nikiforakis N, et al. (2005) Cytokine profile and proteome analysis in bronchoalveolar lavage of patients with sarcoidosis, pulmonary fibrosis associated with systemic sclerosis and idiopathic pulmonary fibrosis. Proteomics 5: 1423-1430.
38. Plymoth A, Lofdahl CG, Ekberg-Jansson A, Dahlback M, Broberg P, et al. (2007) Protein expression patterns associated with progression of chronic obstructive pulmonary disease in bronchoalveolar lavage of smokers. Clin Chem 53: 636-644.
39. Haque R, Umstead TM, Freeman WM, Floros J, Phelps DS (2009) The impact of surfactant protein-A on ozone-induced changes in the mouse bronchoalveolar lavage proteome. Proteome Sci 7: 12.

40. Zhang L, Wang M, Kang X, Boontheung P, Li N, et al. (2009) Oxidative stress and asthma: proteome analysis of chitinase-like proteins and FIZZ1 in lung tissue and bronchoalveolar lavage fluid. J Proteome Res 8: 1631-1638.
41. Carey MA, Bradbury JA, Rebolloso YD, Graves JP, Zeldin DC, et al. (2010) Pharmacologic inhibition of COX-1 and COX-2 in influenza A viral infection in mice. PLoS One 5: e11610.
42. Brown JN, Estep RD, Lopez-Ferrer D, Brewer HM, Clauss TR, et al. (2010) Characterization of macaque pulmonary fluid proteome during monkeypox infection: dynamics of host response. Mol Cell Proteomics 9: 2760-2771.
43. Hosakote YM, Liu T, Castro SM, Garofalo RP, Casola A (2009) Respiratory syncytial virus induces oxidative stress by modulating antioxidant enzymes. Am J Respir Cell Mol Biol 41: 348-357.
44. Ventura CL, Higdon R, Hohmann L, Martin D, Kolker E, et al. (2008) Staphylococcus aureus elicits marked alterations in the airway proteome during early pneumonia. Infect Immun 76: 5862-5872.
45. Ventura CL, Higdon R, Kolker E, Skerrett SJ, Rubens CE (2008) Host airway proteins interact with Staphylococcus aureus during early pneumonia. Infect Immun 76: 888-898.
46. Ali M, Umstead TM, Haque R, Mikerov AN, Freeman WM, et al. (2010) Differences in the BAL proteome after Klebsiella pneumoniae infection in wild type and SP-A-/- mice. Proteome Sci 8: 34.
47. Lok SS, Haider Y, Howell D, Stewart JP, Hasleton PS, et al. (2002) Murine gammaherpes virus as a cofactor in the development of pulmonary fibrosis in bleomycin resistant mice. Eur Respir J 20: 1228-1232.
48. Krug LT, Torres-Gonzalez E, Qin Q, Sorescu D, Rojas M, et al. (2010) Inhibition of NF-kappaB signaling reduces virus load and gammaherpesvirus-induced pulmonary fibrosis. Am J Pathol 177: 608-621.
49. Ebrahimi B, Dutia BM, Brownstein DG, Nash AA (2001) Murine gammaherpesvirus-68 infection causes multi-organ fibrosis and alters leukocyte trafficking in interferon-gamma receptor knockout mice. Am J Pathol 158: 2117-2125.
50. Stoolman JS, Vannella KM, Coomes SM, Wilke CA, Sisson TH, et al. (2010) Latent Infection by Gammaherpesvirus Stimulates Pro-fibrotic Mediator Release from Multiple Cell Types. Am J Physiol Lung Cell Mol Physiol.
51. Veenstra TD, Conrads TP, Hood BL, Avellino AM, Ellenbogen RG, et al. (2005) Biomarkers: mining the biofluid proteome. Mol Cell Proteomics 4: 409-418.
52. Bortz E, Whitelegge JP, Jia Q, Zhou ZH, Stewart JP, et al. (2003) Identification of proteins associated with murine gammaherpesvirus 68 virions. Journal of Virology 77: 13425-13432.
53. Gharib SA, Vaisar T, Aitken ML, Park DR, Heinecke JW, et al. (2009) Mapping the lung proteome in cystic fibrosis. J Proteome Res 8: 3020-3028.
54. Chang DW, Hayashi S, Gharib SA, Vaisar T, King ST, et al. (2008) Proteomic and computational analysis of bronchoalveolar proteins during the course of the acute respiratory distress syndrome. Am J Respir Crit Care Med 178: 701-709.
55. Chen JH, Chang YW, Yao CW, Chiueh TS, Huang SC, et al. (2004) Plasma proteome of severe acute respiratory syndrome analyzed by two-dimensional gel electrophoresis and mass spectrometry. Proc Natl Acad Sci U S A 101: 17039-17044.

doi:10.20944/preprints201809.0008.v1




56. Imai Y, Kuba K, Neely GG, Yaghubian-Malhami R, Perkmann T, et al. (2008) Identification of oxidative stress and Toll-like receptor 4 signaling as a key pathway of acute lung injury. Cell 133: 235-249.
57. Kolliputi N, Waxman AB (2009) IL-6 cytoprotection in hyperoxic acute lung injury occurs via suppressor of cytokine signaling-1-induced apoptosis signal-regulating kinase-1 degradation. Am J Respir Cell Mol Biol 40: 314-324.
58. Conn CA, McClellan JL, Maassab HF, Smitka CW, Majde JA, et al. (1995) Cytokines and the acute phase response to influenza virus in mice. Am J Physiol 268: R78-84.
59. Quinton LJ, Jones MR, Robson BE, Mizgerd JP (2009) Mechanisms of the hepatic acute-phase response during bacterial pneumonia. Infect Immun 77: 2417-2426.
60. Dennis G, Jr., Sherman BT, Hosack DA, Yang J, Gao W, et al. (2003) DAVID: Database for Annotation, Visualization, and Integrated Discovery. Genome Biol 4: P3.
61. Sun J, Druhan LJ, Zweier JL (2010) Reactive oxygen and nitrogen species regulate inducible nitric oxide synthase function shifting the balance of nitric oxide and superoxide production. Arch Biochem Biophys 494: 130-137.
62. Bortz E, Westera L, Maamary J, Steel J, Albrecht RA, et al. (2011) Host- and strain-specific regulation of influenza virus polymerase activity by interacting cellular proteins. mBio 2(4): e00151-1
63. Brown HJ, Song MJ, Deng H, Wu TT, Cheng G, et al. (2003) NF-kappaB inhibits gammaherpesvirus lytic replication. J Virol 77: 8532-8540.
64. Symensma TL, Martinez-Guzman D, Jia Q, Bortz E, Wu TT, et al. (2003) COX-2 induction during murine gammaherpesvirus 68 infection leads to enhancement of viral gene expression. J Virol 77: 12753-12763.
65. Hwang S, Wu TT, Tong LM, Kim KS, Martinez-Guzman D, et al. (2008) Persistent gammaherpesvirus replication and dynamic interaction with the host in vivo. J Virol 82: 12498-12509.
66. Kishimoto T, Akira S, Taga T (1992) IL-6 receptor and mechanism of signal transduction. Int J Immunopharmacol 14: 431-438.
67. Lorenz J, Zahlten J, Pollok I, Lippmann J, Scharf S, et al. (2010) Legionella pneumophila induced i{kappa}b{zeta}-dependent expression of il-6 in lung epithelium. Eur Respir J.
68. Breen EC, Gage JR, Guo B, Magpantay L, Narazaki M, et al. (2001) Viral interleukin 6 stimulates human peripheral blood B cells that are unresponsive to human interleukin 6. Cell Immunol 212: 118-125.
69. Deng H, Chu JT, Rettig MB, Martinez-Maza O, Sun R (2002) Rta of the human herpesvirus 8/Kaposi sarcoma-associated herpesvirus up-regulates human interleukin-6 gene expression. Blood 100: 1919-1921.
70. Qin Z, Kearney P, Plaisance K, Parsons CH (2010) Pivotal advance: Kaposi's sarcoma-associated herpesvirus (KSHV)-encoded microRNA specifically induce IL-6 and IL-10 secretion by macrophages and monocytes. J Leukoc Biol 87: 25-34.
71. Cho HY, Imani F, Miller-DeGraff L, Walters D, Melendi GA, et al. (2009) Antiviral activity of Nrf2 in a murine model of respiratory syncytial virus disease. Am J Respir Crit Care Med 179: 138-150.

72. Kosminder B, Messier EM, Janssen WJ, Nahreini P, Wang J, et al. (2012) Nrf2 protects human alveolar epithelial cells against injury induced by influenza A virus. Resp Res 13: 43.
73. Kumar P, Sharma S, Khanna M, Raj HG (2003) Effect of Quercetin on lipid peroxidation and changes in lung morphology in experimental influenza virus infection. Int J Exp Pathol 84: 127-133.
74. Baskin CR, Garcia-Sastre A, Tumpey TM, Bielefeldt-Ohmann H, Carter VS, et al. (2004) Integration of clinical data, pathology, and cDNA microarrays in influenza virus-infected pigtailed macaques (Macaca nemestrina). J Virol 78: 10420-10432.
75. Suliman HB, Ryan LK, Bishop L, Folz RJ (2001) Prevention of influenza-induced lung injury in mice overexpressing extracellular superoxide dismutase. Am J Physiol Lung Cell Mol Physiol 280: L69-78.
76. Castro SM, Guerrero-Plata A, Suarez-Real G, Adegboyega PA, Colasurdo GN, et al. (2006) Antioxidant treatment ameliorates respiratory syncytial virus-induced disease and lung inflammation. Am J Respir Crit Care Med 174: 1361-1369.
77. Schneider D, Ganesan S, Comstock AT, Meldrum CA, Mahidhara R, et al. (2010) Increased cytokine response of rhinovirus-infected airway epithelial cells in chronic obstructive pulmonary disease. Am J Respir Crit Care Med 182: 332-340.
78. Kavouras JH, Prandovszky E, Valyi-Nagy K, Kovacs SK, Tiwari V, et al. (2007) Herpes simplex virus type 1 infection induces oxidative stress and the release of bioactive lipid peroxidation by-products in mouse P19N neural cell cultures. J Neurovirol 13: 416-425.
79. Mathew SS, Bryant PW, Burch AD (2010) Accumulation of oxidized proteins in Herpesvirus infected cells. Free Radic Biol Med 49: 383-391.
80. Kaul P, Singh I, Turner RB (2002) Effect of rhinovirus challenge on antioxidant enzymes in respiratory epithelial cells. Free Radic Res 36: 1085-1089.
81. Nikolic D, van Breemen RB (2001) DNA oxidation induced by cyclooxygenase-2. Chem Res Toxicol 14: 351-354.
82. Hartshorn KL (2009) Role of surfactant protein A and D (SP-A and SP-D) in human antiviral host defense. Front Biosci (Schol Ed) 2: 527-546.
83. Fisher AB, Dodia C, Chander A (1994) Inhibition of lung calcium-independent phospholipase A2 by surfactant protein A. Am J Physiol 267: L335-341.
84. Manevich Y, Fisher AB (2005) Peroxiredoxin 6, a 1-Cys peroxiredoxin, functions in antioxidant defense and lung phospholipid metabolism. Free Radic Biol Med 38: 1422-1432.
85. Fisher AB, Dodia C, Yu K, Manevich Y, Feinstein SI (2006) Lung phospholipid metabolism in transgenic mice overexpressing peroxiredoxin 6. Biochim Biophys Acta 1761: 785-792.
86. Liu G, Feinstein SI, Wang Y, Dodia C, Fisher D, et al. (2010) Comparison of glutathione peroxidase 1 and peroxiredoxin 6 in protection against oxidative stress in the mouse lung. Free Radic Biol Med 49: 1172-1181.
87. Bocchino M, Agnese S, Fagone E, Svegliati S, Grieco D, et al. (2010) Reactive oxygen species are required for maintenance and differentiation of primary lung fibroblasts in idiopathic pulmonary fibrosis. PLoS One 5: e14003.
88. Mazur W, Lindholm P, Vuorinen K, Myllarniemi M, Salmenkivi K, et al. (2010) Cell-specific elevation of NRF2 and sulfiredoxin-1 as markers of oxidative stress in the lungs of idiopathic pulmonary fibrosis and non-specific interstitial pneumonia. APMIS 118: 703-712.

Preprints (www.preprints.org) | NOT PEER-REVIEWED | Posted: 3 September 2018 doi:10.20944/preprints201809.0008.v1



89. Vuorinen K, Ohlmeier S, Lepparanta O, Salmenkivi K, Myllarniemi M, et al. (2008) Peroxiredoxin II expression and its association with oxidative stress and cell proliferation in human idiopathic pulmonary fibrosis. J Histochem Cytochem 56: 951-959.
90. Lee S, Salwinski L, Zhang C, Chu D, Sampankanpanich C, et al. (2011) An integrated approach to elucidate the intra-viral and viral-cellular protein interaction networks of a gamma-herpesvirus. PLoS Pathog 7: e1002297.
91. Rodrigues L, Filipe J, Seldon MP, Fonseca L, Anrather J, et al. (2009) Termination of NF-kappaB activity through a gammaherpesvirus protein that assembles an EC5S ubiquitin-ligase. EMBO J 28: 1283-1295.
92. Li X, Feng J, Sun R (2011) Oxidative stress induces reactivation of Kaposi's sarcoma-associated herpesvirus and death of primary effusion lymphoma cells. J Virol 85: 715-724.
93. Monton C, Torres A (1998) Lung inflammatory response in pneumonia. Monaldi Arch Chest Dis 53: 56-63.
94. de Jong HK, van der Poll T, Wiersinga WJ (2010) The systemic pro-inflammatory response in sepsis. J Innate Immun 2: 422-430.
95. Kramer HB, Lavender KJ, Qin L, Stacey AR, Liu MK, et al. (2010) Elevation of intact and proteolytic fragments of acute phase proteins constitutes the earliest systemic antiviral response in HIV-1 infection. PLoS Pathog 6: e1000893.
96. Morgan K, Kalsheker NA (1997) Regulation of the serine proteinase inhibitor (SERPIN) gene alpha 1-antitrypsin: a paradigm for other SERPINs. Int J Biochem Cell Biol 29: 1501-1511.
97. Akira S, Kishimoto T (1992) IL-6 and NF-IL6 in acute-phase response and viral infection. Immunol Rev 127: 25-50.
98. Fasnacht N, Muller W (2008) Conditional gp130 deficient mouse mutants. Semin Cell Dev Biol 19: 379-384.
99. Martinez Cordero E, Gonzalez MM, Aguilar LD, Orozco EH, Hernandez Pando R (2008) Alpha-1-acid glycoprotein, its local production and immunopathological participation in experimental pulmonary tuberculosis. Tuberculosis (Edinb) 88: 203-211.
100. Naylor HM, Newcomer ME (1999) The structure of human retinol-binding protein (RBP) with its carrier protein transthyretin reveals an interaction with the carboxy terminus of RBP. Biochemistry 38: 2647-2653.
101. Isaacs CE, Xu W, Pullarkat RK, Kascsak R (2000) Retinoic acid reduces the yield of herpes simplex virus in Vero cells and alters the N-glycosylation of viral envelope proteins. Antiviral Res 47: 29-40.
102. Caselli E, Galvan M, Santoni F, Alvarez S, de Lera AR, et al. (2008) Retinoic acid analogues inhibit human herpesvirus 8 replication. Antivir Ther 13: 199-209.
103. Cui D, Moldoveanu Z, Stephensen CB (2000) High-level dietary vitamin A enhances T-helper type 2 cytokine production and secretory immunoglobulin A response to influenza A virus infection in BALB/c mice. J Nutr 130: 1132-1139.
104. Tabata C, Kadokawa Y, Tabata R, Takahashi M, Okoshi K, et al. (2006) All-trans-retinoic acid prevents radiation- or bleomycin-induced pulmonary fibrosis. Am J Respir Crit Care Med 174: 1352-1360.

 doi:10.20944/preprints201809.0008.v1



105. Tabata C, Kubo H, Tabata R, Wada M, Sakuma K, et al. (2006) All-trans retinoic acid modulates radiation-induced proliferation of lung fibroblasts via IL-6/IL-6R system. Am J Physiol Lung Cell Mol Physiol 290: L597-606.

106. Sun H, Gong S, Carmody RJ, Hilliard A, Li L, et al. (2008) TIPE2, a negative regulator of innate and adaptive immunity that maintains immune homeostasis. Cell 133: 415-426.

107. E X, Hwang S, Oh S, Lee JS, Jeong JH, et al. (2009) Viral Bcl-2-mediated evasion of autophagy aids chronic infection of gammaherpesvirus 68. PLoS Pathog 5: e1000609.

108. Rahman I (2005) Oxidative stress in pathogenesis of chronic obstructive pulmonary disease: cellular and molecular mechanisms. Cell Biochem Biophys 43: 167-188.

109. Brown JN, Palermo RE, Baskin CR, Gritsenko M, Sabourin PJ, et al. (2010) Macaque proteome response to highly pathogenic avian influenza and 1918 reassortant influenza virus infections. J Virol 84: 12058-12068.

110. Bortz E, Wang L, Jia Q, Wu TT, Whitelegge JP, et al. (2007) Murine gammaherpesvirus 68 ORF52 encodes a tegument protein required for virion morphogenesis in the cytoplasm. J Virol 81: 10137-10150.

111. Wu TT, Liao HI, Tong L, Leang RS, Smith G, et al. (2011) Construction and characterization of an infectious murine gammaherpesivrus-68 bacterial artificial chromosome. J Biomed Biotechnol 2011: 926258.

112. May JS, Coleman HM, Boname JM, Stevenson PG (2005) Murine gammaherpesvirus-68 ORF28 encodes a non-essential virion glycoprotein. J Gen Virol 86: 919-928.

113. Jia Q, Chernishof V, Bortz E, McHardy I, Wu TT, et al. (2005) Murine gammaherpesvirus 68 open reading frame 45 plays an essential role during the immediate-early phase of viral replication. J Virol 79: 5129-5141.

114. Gomez SM, Bil KY, Aguilera R, Nishio JN, Faull KF, et al. (2003) Transit peptide cleavage sites of integral thylakoid membrane proteins. Mol Cell Proteomics 2: 1068-1085.

115. Shoemaker LD, Orozco NM, Geschwind DH, Whitelegge JP, Faull KF, et al. (2010) Identification of differentially expressed proteins in murine embryonic and postnatal cortical neural progenitors. PLoS One 5: e9121.

116. Palagi PM, Lisacek F, Appel RD (2009) Database interrogation algorithms for identification of proteins in proteomic separations. Methods Mol Biol 519: 515-531.

117. Benjamini Y, Drai D, Elmer G, Kafkafi N, Golani I (2001) Controlling the false discovery rate in behavior genetics research. Behav Brain Res 125: 279-284.

118. Katoh K, Kuma K, Toh H, Miyata T (2005) MAFFT version 5: improvement in accuracy of multiple sequence alignment. Nucleic Acids Res 33: 511-518.